Published in : Computer Methods and Programs in Biomedicine (2019), n°175, pp. 129-137
DOI: 10.1016/j.cmpb.2019.04.017
Status : Postprint (Author's version)

FRACTAL DIMENSION ANALYSIS OF STATES OF CONSCIOUSNESS AND UNCONSCIOUSNESS USING TRANSCRANIAL MAGNETIC STIMULATION

J. Ruiz de Miras [a], F. Soler [b], S. Iglesias-Parro [c], A.J. Ibânez-Molina [c], A.G. Casali [d], S. Laureys [e], M. Massimini [f,g], FJ. Esteban [h], J. Navas [i], J.A. Langa [j]

[a] *Computer Science Department, University of Jaén, Jaén, Spain*

[b] *Department of Philosophy, Logic and Philosophy of Science, University of Sevilla, Sevilla, Spain*

[c] *Department of Psychology, University of Jaén, Jaén, Spain*

[d] *Institute of Science and Technology, Federal University of Sao Paulo, S!o José dos Campos, Brazil*

[e] *Coma Science Group, GIGA Consciousness Research Centre and Neurology Department, University and University Hospital of Liège, Belgium*

[f] *Department of Biomedical and Clinical Sciences "Luigi Sacco", University of Milan, Milano, Italy*

[g] *RCCS Fondazione Don Carlo Gnocchi, Milan, Italy*

[h] *Department of Experimental Biology, University of Jaén, Jaén, Spain*

[i] *Department of Mathematics, University of Jaén, Jaén, Spain*

[j] *Department of Differential Equations and Numerical Analysis, University of Sevilla, Sevilla, Spain*

KEYWORDS:

Fractal dimension

EEG

Transcranial magnetic stimulation Consciousness

ABSTRACT

Background and objective: Knowing whether a subject is conscious or not is a current challenge with a deep potential clinical impact. Recent theoretical considerations suggest that consciousness is linked to the complexity of distributed interactions within the corticothalamic system. The fractal dimension (FD) is a quantitative parameter that has been extensively used to analyse the complexity of structural and functional patterns of the human brain. In this study we investigate FD to assess whether it can discriminate between consciousness and different states of unconsciousness in healthy individuals.

Methods: We study 69 high-density electroencephalogram (hd-EEG) measurements after transcranial magnetic stimulation (TMS) in 18 healthy subjects progressing from wakefulness to non-rapid eye movement (NREM) sleep and sedation induced by different anaesthetic agents (xenon and propofol). We quantify the integration of thalamocortical networks by calculating the FD of a spatiotemporal voxelization obtained from the locations of all sources that are significantly activated by the perturbation (4DFD). Moreover, we study the temporal evolution of the evoked spatial distributions and compute a measure of the differentiation of the response

Published in : Computer Methods and Programs in Biomedicine (2019), n°175, pp. 129-137
DOI: 10.1016/j.cmpb.2019.04.017
Status : Postprint (Author's version)

by means of the Higuchi FD (HFD). Finally, a Fractal Dimension Index (FDI) of perturbational complexity is computed as the product of both quantities: integration FD (4DFD) and differentiation FD (HFD).

Results: We found that FDI is significantly lower in sleep and sedation when compared to wakefulness and provides an almost perfect intra-subject discrimination between conscious and unconscious states. Conclusions: These results support the combination of FD measures of cortical integration and cortical differentiation as a novel paradigm of tracking complex spatiotemporal dynamics in the brain that could provide further insights into the link between complexity and the brain's capacity to sustain consciousness.

1. Introduction

Determining the level of consciousness is a challenging task with many clinical applications [1,2]. A number of methods have been proposed for a non-invasive assessment of the level of consciousness, mainly from electroencephalogram (EEG) signal analysis [3-6]. These methods are especially useful in patients where clinical tests such as the Coma Recovery Scale-Revised (CRS-R) [7] may fail in detecting consciousness due to patient's lack of ability to respond to a sensory stimulus. Some of these methods are focused on the spectral analysis of the resting EEGs [8], other methods have been developed to capture the connectivity patterns of multiple EEG sites [9], and there are also methods based on the analysis of the event-related potentials (ERP) from simple stimuli that change their trace depending on the conscious stage of the participant [10]. When combined, these measures can synergize to allow an automatic classification of patients' state of consciousness [5,6]. Although these methodological tools can achieve a good level of discrimination, most of them need further refinement and a clear theoretical background. One promising approach is to explore the informational or complexity content of the EEG signals during conscious/unconscious states [11]. As examples, detrended fluctuation analysis, entropies and complexity estimators for monitoring depth of anaesthesia have been explored [12-14]. One noteworthy recent approach is the development of a perturbational complexity index (PCI) in the clinical assessment of brain-injured, unresponsive patients [15,16]. This indicator is theoretically based on the Integrated Information Theory (IIT) of consciousness [17,18]. IIT argues that the brain should be able to sustain consciousness to the extent that it can enter several different states (differentiation) as a causal integrated whole (integration). PCI was designed to capture this balance between differentiation and causal integration. In short, the index quantifies the algorithmic complexity (differentiation) of the spatiotemporal propagation of EEG activity after transcranial magnetic stimulation (causal integration). Although PCI has been shown to be highly reliable to assess conscious states at a single patient level [16], efforts have been made to increase its classification accuracy [2] and a complete understanding of the link between PCI and theoretical measures of complexity in the brain is still lacking.

In the present study we further explore the perturbational approach introduced in [15], using the fractal dimension (FD) as the reference measure in order to obtain a complexity estimation. FD is a measure of the complexity of a set and so, in particular, of a data set obtained from the internal dynamics on such a complex system as the brain [19]. Indeed, FD is a quantitative

Published in : Computer Methods and Programs in Biomedicine (2019), n°175, pp. 129-137
DOI: 10.1016/j.cmpb.2019.04.017
Status : Postprint (Author's version)

parameter that is extensively used to analyse medical signals in fields such as neuroimaging, bone texture, mammography and electrocardiogram/electroencephalogram-based diagnosis, among others [20]. Metrics of FD are able to characterize the complexity of a wide range of signals of interest by assessing how a fractal structure occupies their geometrical target space [21]. The versatility of FD analysis applied to EEG has enabled the development of a remarkable number of applications in several diseases such as epilepsy [22], sleeping disorders [23] and Alzheimer's disease [24].

From a theoretical point of view, when we define a dynamical system on a physical substrate (in our case, dynamics on a complex system describing a network in the brain), the natural object to describe its asymptotic behaviour is the global attractor, which seems to be behind some functionality properties of the brain [25-27]. A global attractor can be characterized as a new complex network, determining all the asymptotic dynamics of a system [28,29]. By its informational nature they have been defined as Informational Structures [30], allowing for a continuous and dynamical approach to the integrated information in IIT. Note that attractors are commonly described as fractal sets [31], their fractal dimension being just an index of their complexity, usually associated to chaotic dynamics. Thus, phenomenological measures of fractality from real data should be related to the complexity of informational structures, which we hope are in the base of a theoretical approach to the description of conscious states (see Section 4).

There exists little previous work studying the fractal structure of the brain activity present in the different levels of consciousness. To the best of our knowledge, the first study on FD and consciousness was presented by Nan et al. in [32]. They analysed the FD, computed as the correlation dimension [33], of the EEG signals measured in three different moments during the realization of a task in the conscious state. They found that FD of EEG may quickly respond to the changes in mental states. Solhjoo et al. compared mental task classification in hypnosis and normal states through FD of EEG signal [34]. In this study, Higuchi FD (HFD) [35] performed very well and better than Petrosian FD [36] in classifying the mental tasks. HFD of EEG was also tested as a measure of depth of anaesthesia and sedation in [12]. An interesting conclusion of this study is that the EEG window length processed has an influence on the results, with window lengths needed of at least 20s in order to obtain reliable results. More recently, Ibáñez et al. [37] proposed the use of FD to characterize the complexity of the EEG signal associated with internally and externally generated conscious experiences. Ibáñez et al.'s study is also based on the HFD of the EEG signals and they showed that non-linear EEG complexity expressed by means of HFD can be a reliable measure of the neural correlates of consciousness. However, none of these previous studies have addressed the problem of how to use FD to discriminate between consciousness and unconsciousness.

In this paper we study the fractal structure of the brain activity in several consciousness states in a novel way. Specifically, we compute the 4D FD of the brain's early reaction (within the first 130 ms) to the direct TMS-induced cortical perturbation and use the HFD to measure the variability of the complexity of that reaction over time. By combining 4DFD (integration) and HFD (differentiation) we introduce the FDI, a novel empirical measure of brain complexity in response to a direct cortical perturbation. We tested FDI on a data set of TMS-evoked potentials

Published in : Computer Methods and Programs in Biomedicine (2019), n°175, pp. 129-137
DOI: 10.1016/j.cmpb.2019.04.017
Status : Postprint (Author's version)

recorded from healthy subjects during wakefulness, non-rapid eye movement (NREM) sleep, and different levels of sedation induced by the anaesthetics xenon and propofol.

2. Methods

2.1. SUBJECTS

We included 69 TMS/EEG measurements in 18 healthy subjects in this study. This data set was recorded in previously-published studies. Specifically, the data on sleep (subjects 1 to 6) were derived from studies by Massimini et al. [38,39], and the data from xenon anaesthesia (subjects 7 to 12) and propofol sedation (subjects 13 to 18) were derived from a study by Casali et al. [15].

2.2. TMS/EEG ACQUISITION

The technical details of the procedures for the acquisition of the data set were described in prior publications [15,38,39]. In this section those procedures are briefly described.

2.2.1. WAKEFULNESS AND SLEEP (SUBJECTS 1-6)

TMS/EEG data was collected in six healthy subjects (subjects 1¬6, six males, age ranging from 24 to 34). The first TMS-EEG session was acquired while the subjects were alert and relaxed, with their eyes open. Stimuli resulted in an electric field at the cortical target (Brodmann area 6, BA6) of about 90 V/m. A second TMS-EEG session was recorded, with the same stimulation intensity, after subjects entered a consolidated period of NREM sleep stage 3. In four of the six subjects (subjects 3 to 6), a third session was also recorded in which TMS was delivered at higher intensity (160 V/m) to the midline sensorimotor cortex (BA4).

2.2.2. WAKEFULNESS AND ANAESTHESIA (SUBJECTS 7-18)

Six healthy volunteers (two males, four females; age ranging 18 to 28) were administered xenon anaesthesia (subjects 7-12). The first TMS-EEG session was recorded during wakefulness with stimuli targeted over the right motor cortex (BA4) at an intensity of about 100 V/m while subjects were lying on a bed with their eyes open. During a 40-min period, xenon was introduced progressively. Subjects received between 24 and 32 l of xenon in total [15]. Stimulations with the same parameters as for wakefulness were then performed during loss of consciousness (level 1 of the Modified Observer's Assessment of Alertness and Sedation, MOAAS, ranging from 5, Awake to 1, Unresponsive).

Finally, another six healthy volunteers (three males, three females; age ranging from 20 to 27) were administered propofol anaesthesia (subjects 13-18). TMS-EEG measurements were performed first during wakefulness while subjects were lying on a bed with their eyes open and

Published in : Computer Methods and Programs in Biomedicine (2019), n°175, pp. 129-137
DOI: 10.1016/j.cmpb.2019.04.017
Status : Postprint (Author's version)

then during an intermediate level of sedation (levels 2 to 3 of the MOAAS) followed by anaesthesia with loss of consciousness (level 1 of the MOAAS). Across these conditions, TMS was targeted over the motor (BA4), premotor (BA6), parietal (BA7) and occipital (BA19) areas at an intensity of about 110 V/m. Propofol anesthesia was obtained with a computer- controlled intravenous infusion of propofol to obtain constant effect-site concentrations (Alaris TIVA; CareFusion). The propofol plasma and effect-site concentrations were estimated with a three-compartment pharmacokinetic model [15].

2.3. EXTRACTING THE DETERMINISTIC PATTERNS OF CORTICAL ACTIVATION

As described in [38,40], TMS-evoked potentials were recorded with a 60-channel TMS-compatible EEG amplifier, and stimuli were delivered by means of a Focal Bipulse 8-Coil, driven by a Mobile Stimulator Unit and combined with a magnetic resonance- guided navigation system that employs a 3D infrared tracking position sensor unit to map the positions of TMS coil and subject's head within the reference space of individual structural magnetic resonance imaging (MRI). The reproducibility of the stimulation coordinates across sessions was guaranteed by a virtual aiming device that indicated in real-time any deviation from the desired target greater than 3 mm. Then the primary electromagnetic sources of scalp EEG activity were localized by performing source modelling as detailed in previous analyses of TMS/EEG [40]. First, conductive head volume was modelled according to the 3-spheres BERG method [41,42] as implemented in the Brainstorm software package (http://neuroimage.usc.edu/brainstorm). These three concentric spheres represented the best-fitting spheres of inner skull, outer skull and scalp compartments extracted from individual MRIs. The solution space was constrained to the cerebral cortex that was modelled as a three-dimensional grid of 3004 fixed dipoles oriented normally to cortical surface. This model was adapted to the anatomy of each subject using the Statistical Parametric Mapping (SPM) software package (https://www.fil.ion.ucl.ac.uk/spm). Finally, the inverse problem of determining the distribution of electrical sources in the brain was solved by the Weighted Minimum Norm constraint applied to an empirical Bayesian approach [43-45] as implemented in SPM.

After source modelling, the deterministic responses of the brain were estimated by applying a statistical procedure to TMS-evoked cortical currents based on a nonparametric bootstrap procedure [15]. A binary spatiotemporal distribution of significant sources SS(x,t) was then calculated, where SS(x,t) = 1 for significant sources x and time samples t; and SS(x,t) = 0 otherwise. Fig. 1 outlines this binarization process.

2.4. FRACTAL DIMENSION INDEX COMPUTATION

After performing the binarization process to extract the matrix of significant sources, SS(x,t), which describes the spatiotemporal pattern of activation caused by the TMS perturbation, the next step consisted of computing a Fractal Dimension Index (FDI) based on the complexity of the sources' spatiotemporal distributions.

The fractal dimension (FD) of an ideal fractal set $S \in \mathrm{R}\ d$ can be calculated by means of the box-counting method as follows [21]:

Published in : Computer Methods and Programs in Biomedicine (2019), n°175, pp. 129-137
DOI: 10.1016/j.cmpb.2019.04.017
Status : Postprint (Author's version)

$$FD(S) = \frac{\log(N_r)}{\log\left(\frac{1}{r}\right)} \quad (1)$$

where Nr is the number of boxes of size r^d that are required to completely cover the fractal set S. However, when that set is not an ideal fractal then the FD value is obtained as the linear regression of log(Nr) against log (1/r) for several values of r.

We started from the point cloud described by the 3D localizations associated to the significant sources at each time sample (see Fig. 2.A-C). We then computed the 3DFD of each point cloud by using the box-counting method [46] (d = 3 in Eq. (1)). A grid of 256 x 256x 256 voxels was defined covering each point cloud (see Fig. 2.D, box size r = 256) and it was successively divided by 2 until reaching a size of 1 x 1 x 1 voxels (Fig. 2.D, box size r = 1). Those voxels in each grid that contain any point of the point cloud define a voxelization for that point cloud, and the number of voxels, Nr, in each voxelization of size r corresponds to the box-counting of the point cloud. Then the 3DFD value is calculated as the slope of the linear piece of the regression line for the log-log plot of Nr vs. 1/r (see Fig. 2.D). In this study, that linear piece corresponds to box sizes ranging from r = 16 to r = 128 (correlation: n = 3105, mean = 0.995, standard deviation = 0.009; see red line in Fig. 2.D). The whole process for calculating the 3DFD values was computed in MATLAB R2013a as described in [47].

In order to obtain a fractal measure of spatiotemporal integration in the thalamocortical networks that are engaged by the perturbation we extended the same algorithm previously described for the 3D case and included time as a fourth dimension, resulting in a 4DFD value of the significant sources spatial distributions (d = 4 in Eq. (1)). The units of the voxels in the fourth dimension correspond to the time samples. In this way, a 4D voxel of size r x r x r x r belongs to the 4D voxelization of size r if any of the r 3D voxels of size r x r x r contains at least one point belonging to one of the point clouds defined at those r time samples. Fig. 3 shows the log-log plot and the 4DFD obtained from the locations of the significant sources in the first 130 ms for a subject awake. As in the case of 3DFD computations, the linear piece of the log-log plot whose slope determines the 4DFD value corresponds to box sizes ranging from r = 16 to r = 128 (correlation: n = 69, mean = 0.996, standard deviation = 0.003; see red line in Fig. 3).

Furthermore, in order to obtain a fractal measure of the differentiation of the TMS-evoked response, we applied the Higuchi method (HFD) to the signals described by the 3DFD time-series (Fig. 4). Higuchi's algorithm calculates FD as follows [35]:

From a given signal s = {r(1), s(2), ..., s(N)}, k curves s_m^k are constructed as:

$$L_m(k) = \frac{\left(\sum_{i=1}^{\left\lfloor \frac{N-m}{k} \right\rfloor} |s(m+ik) - s(m+(i-1)k)|\right) \cdot \frac{N-1}{\left\lfloor \frac{N-m}{k} \right\rfloor k}}{k} \quad (2)$$

where m and k are integers and they indicate the initial time and the time interval, respectively. The length $L_m(k)$ of each curve s_m^k is calculated as:

Published in : Computer Methods and Programs in Biomedicine (2019), n°175, pp. 129-137
DOI: 10.1016/j.cmpb.2019.04.017
Status : Postprint (Author's version)

$$s_m^k = \left\{ s(m), s(m+k), \ldots, s\left(m + \left\lfloor \frac{N-m}{k} \right\rfloor k\right) \right\} m = 1, 2, \ldots, k \quad (3)$$

The length of the curve for time interval k, L(k), is calculated as the average of the m curves $L_m(k)$ for m = 1, ..., k. If $L(k) \alpha k^{-D}$, then the signal s is fractal-like with the dimension D.

Sources Activity

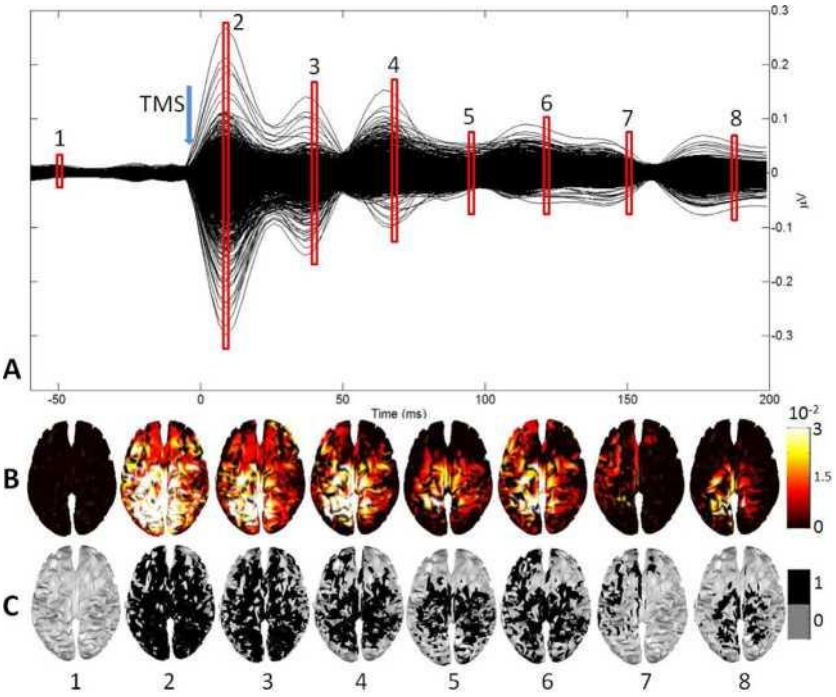

Fig. 1. (A) Sources activity before and after TMS for a subject awake. (B) 3D representation of absolute values of significant sources at eight different time samples. (C) 3D representation of significant sources at those eight time samples after binarization.

Published in : Computer Methods and Programs in Biomedicine (2019), n°175, pp. 129-137
DOI: 10.1016/j.cmpb.2019.04.017
Status : Postprint (Author's version)

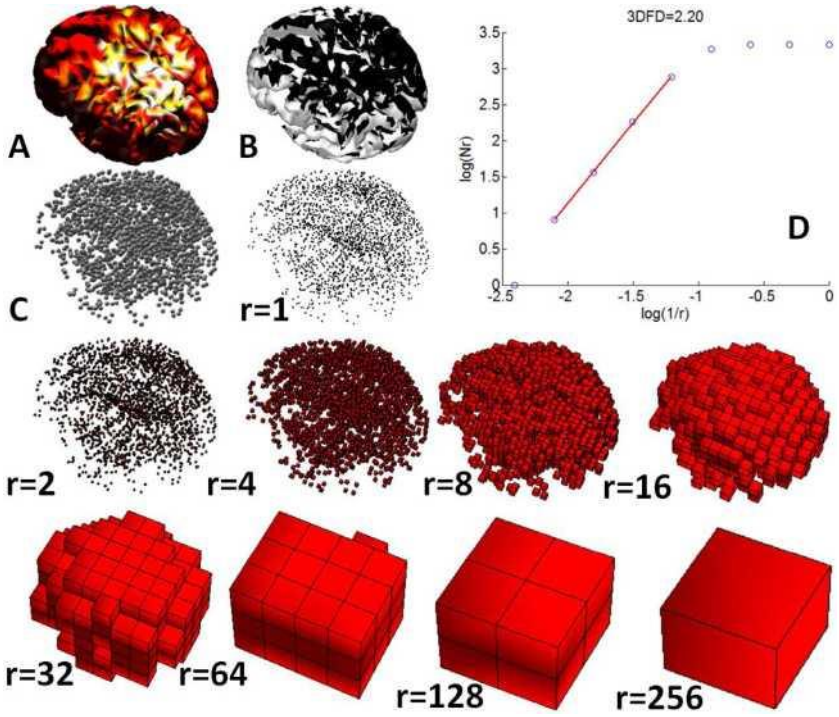

Fig. 2. (A) Significant source activity at the time sample 40 ms after TMS for a subject awake. (B) Binarized sources at that time. (C) Point cloud defined by binarized sources. (D) Log-log plot of number of boxes (Nr) vs. 1/r for voxelizations of the point cloud with box sizes ranging from r = 1 to r = 256. 3DFD value (2.20) is computed as the slope of the linear regression considering the range of sizes from r = 16 to r = 128 (correlation = 0.99). (For interpretation of the references to color in this figure legend, the reader is referred to the web version of this article.)

HFD values of the signals s = 3DFD(t) were computed in MATLAB R2013a using the software written by Selvam and Nadu [48]. Higuchi's algorithm needs a manual-set parameter, kmax, in order to establish the maximum size of the intervals to consider for approximating the signal. To choose the appropriate value of kmax, we computed the HFD values for the range of kmax from 1 to the number of time samples/2 and plotted them against kmax. The value of kmax at which the HFD value plateaus must be selected [49,50]. In the present study most of the subject's data presented that plateau at a value of kmax = 9, so this value was chosen. Fig. 4 shows the HFD values of the 3DFD curves for the three different states of subject 4.

Fig. 4 also shows an important issue regarding the time pe¬riod used in the fractal analysis. Xenon and propofol sessions of subjects 7 and 16, respectively, present segments in the 3DFD curve with a constant value of 0. Moreover, for the case of some propofol sessions in subject 16, those 0-valued segments in the 3DFD curve start and even continue till the end of the curve. This fact occurs because in those time periods no source is significantly activated and therefore the 3DFD value equals 0. It is relevant to minimize the effect of those segments on the HFD computations since a curve with large 0-valued segments would lose its fractal features and therefore its HFD value would also lose its meaning. In this sense, our strategy consisted of calculating the average time in sleeping sessions where large 0-valued segments start, and restricting the 4DFD and HFD computations to this time period for all sessions. As shown previously (Figs. 3 and 4) the average time was established at 130 ms.

Published in : Computer Methods and Programs in Biomedicine (2019), n°175, pp. 129-137
DOI: 10.1016/j.cmpb.2019.04.017
Status : Postprint (Author's version)

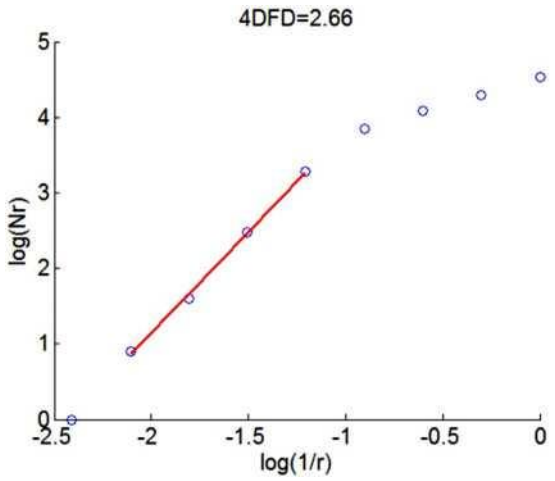

Fig. 3. Log-log plot of number of boxes (Nr) vs. 1/r for 4D voxelizations of the point clouds in the first 130 ms with box sizes ranging from r = 1 to r=256 for a subject who is awake. 4DFD value (2.66) is computed as the slope of the linear regression considering the range of sizes from r = 16 to r = 128 (correlation = 0.99). (For interpretation of the references to color in this figure legend, the reader is referred to the web version of this article.)

Finally, by using the fractal analysis based on 4DFD and HFD we define FDI as follows: let SS(x,t) be the matrix with the binary values (1 or 0) for the sources x at the time samples t for the first 130 ms; let 4DFD be the 4D FD value for the 4D matrix defined by the point clouds made up of 3D locations of sources x with SS(x,t) = 1 for all time samples t (the fourth dimension); let 3 DFD(t) be the vector with the 3DFD values for the point clouds defined by locations of sources x at each time sample t with SS(x,t) = 1; and let HFD be the Higuchi Fractal Dimension value of 3DFD(r). Then we define the Fractal Dimension Index (FDI) of SS(x,t) as the product 4DFD*HFD, which combines, in a single number, the complexity of the temporally integrated spatial distributions (4DFD) and the variability of these distributions (HFD) after the perturbation As an example, for the case of subject 4 in Fig. 4, we obtained the following FDI values: Awake state: 4DFD = 2.71, HFD = 1.60, FDI = 4.35; Asleep 90 state: 4DFD = 2.27, HFD = 1.50, FDI = 3.43; Asleep 160 state: 4DFD = 2.70, HFD = 1.36, FDI = 3.68.

2.5. STATISTICAL ANALYSIS

The effects of the subject's conditions and stimulation parameters on FDI values were estimated using a linear mixed model [51]. Due to unbalanced data design, in order to obtain a bias-free estimation for variance components the model parameters were estimated by means of the Restricted Maximum Likelihood (ReML) method [52]. Null hypotheses were tested with type III F statistics and rejected if $p < 0.05$. FDI values were initially modelled including fixed factors associated with stimulation site, stimulation intensity, and a binary classifier of the subject's conditions (wake-fulness/loss of consciousness). The model also included a random factor associated with the intercept for each subject in order to deal with the unbalanced repeated measures and a random subject-specific effect of loss of consciousness. This additional random factor allows the variance of FDI during wakefulness to differ from that during loss of consciousness. Because no significant effects of the stimulation parameters were observed, the model was restricted to the random factors and a single categorical fixed factor with one level

Published in : Computer Methods and Programs in Biomedicine (2019), n°175, pp. 129-137
DOI: 10.1016/j.cmpb.2019.04.017
Status : Postprint (Author's version)

for each conscious state. Then statistical differences between groups in FDI values were assessed using an analysis of variance (ANOVA), and a post-hoc Bonferroni test at a significance level $\alpha = 0.05$ was performed in order to correct the p-values for multiple comparisons and identify which of the pair of groups are significantly different from each other [53].

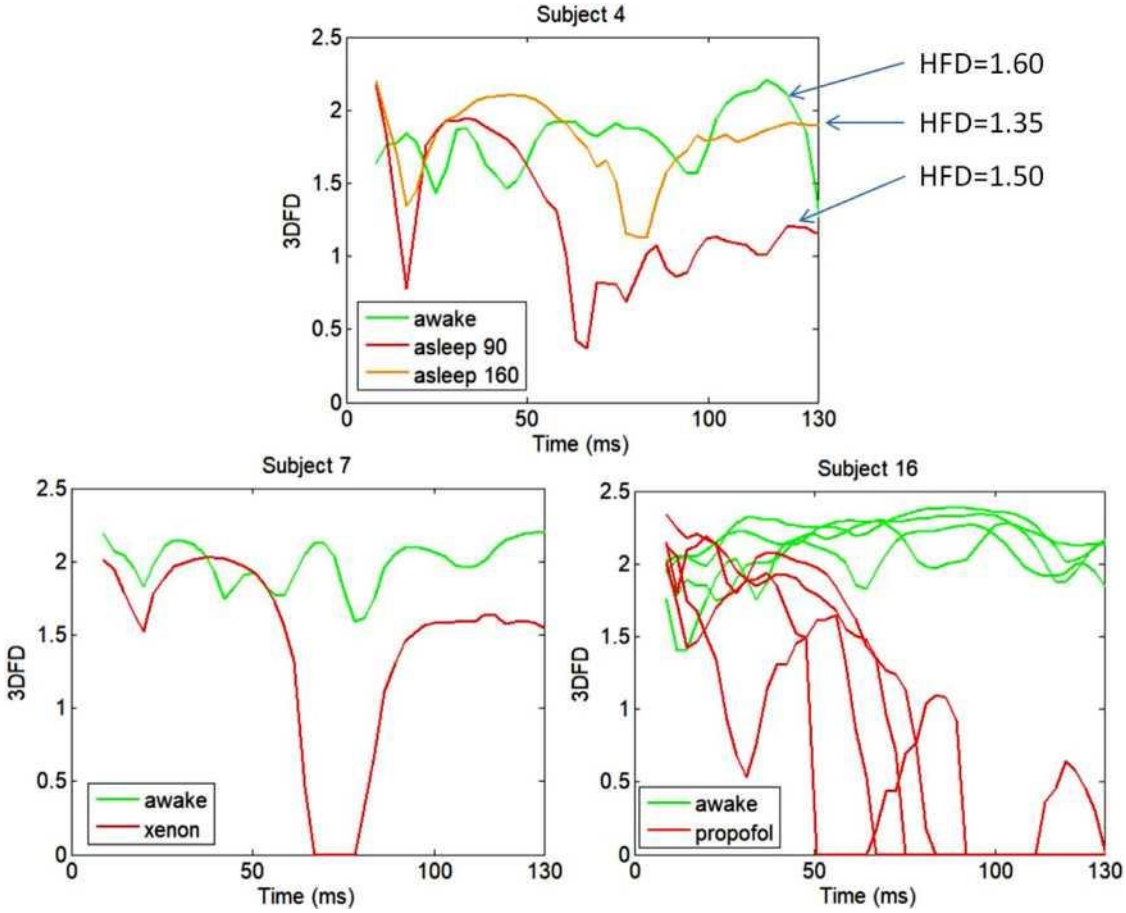

Fig. 4. 3DFD evolution from t=8 ms to t = 130 ms after TMS for three subjects in different states: awake, asleep with a TMS of 90 V/m, asleep with a TMS of 160 V/m, xenon sedated and propofol sedated. Higuchi FD values are also shown for the curves described by the 3DFD evolutions of the three states of subject 4. Subject 16 shows four different sessions in an awake state and another four different sessions with propofol sedation.

The performance of FDI as a classifier was assessed using a receiver operating characteristic (ROC) curve analysis. In this ROC analysis, the proportion of true positive rate (i.e., sensitivity) was plotted against the proportion of false positive rate (i.e., 1- specificity) at different levels of cumulative FDI values [54]. Then, the area under ROC curve (AUC) was computed as an effective measure of the FDI classifier accuracy in ROC curve analysis [55]. ROC analysis was also used to define the optimal cut-off values in order to discriminate between consciousness and unconsciousness based on the FDI value [56]. To determine this optimal cut-off value objectively, we calculated the ROC curve point at which average misclassification costs were minimized by moving a straight line with slope

Published in : Computer Methods and Programs in Biomedicine (2019), n°175, pp. 129-137
DOI: 10.1016/j.cmpb.2019.04.017
Status : Postprint (Author's version)

$S = \frac{Cost\,(P|N)}{Cost\,(N|P)} * \frac{N}{P}$ from the upper left corner of the Cost(N|P)

ROC plot to the bottom right corner, until it intersected the ROC curve [57], where Cost(N|P) is the cost of misclassifying a positive class as a negative class, Cost(P|N) is the cost of misclassifying a negative class as a positive class, with P = number of true positives + number of false negatives and N = number of true negatives + number of false positives being the total instance counts in the positive and negative class, respectively.

All analyses were performed using statistical functions within MATLAB R2013a (The MathWorks Inc., Natick, MA, US).

3. Results

Isolated results for 4DFD and HFD are shown in Figs. 5 and 6, respectively. Both measures present, in general, lower values when subjects were sleeping or sedated.

Fig. 7 shows the FDI values computed for the 69 TMS/EEG. In general, FDI values for measurements in wakefulness are higher than in NREM sleep, and during general anaesthesia with xenon and propofol. The ROC curve analysis described below resulted in an FDI value of 3.73 as the optimal cut-off to discriminate between consciousness and unconsciousness for this data set. In addition, for each subject FDI values in wakefulness are always higher than FDI values in unconsciousness, except for the case of a certain measurement on subject 5.

We tested the effects of stimulation site [superior occipital gyrus (BA19), superior parietal gyrus (BA7), rostral portion of the premotor cortex (BA6), and midline sensorimotor cortex (BA4)] and intensity (induced field on the cortical surface: 90 V/m, 100 V/m, and 110 V/m) on FDI. When included as fixed factors in a linear mixed model, stimulation sites and stimulation intensities did not have significant effects on FDI values ($F = 0.58$, $p = 0.67$ for sites and $F = 0.87$, $p = 0.43$ for intensities).

After comparing the FDI scores of sessions grouped by conscious state (see Table 1), we found that unconscious groups display significant reductions ($F=38.43$, $p = 2.09x10\text{-}14$) in their FDI values regarding the conscious group (see Fig. 8). The values of T and p for group comparison after Bonferroni's multiple comparisons correction in Fig. 8 are: $T = 6.00$, $p = 2.89x10\text{-}7$ (awake - asleep), $T = 6.35$, $p = 6.94x10\text{-}8$ (awake - xenon), and $T = 9.46$, $p = 2.27\ x10\text{-}13$ (awake - propofol). No significant differences were found between pairs of unconscious groups in FDI.

The performance as a classifier of FDI through ROC curve analysis is shown in Fig. 9. In this analysis an AUC of 0.966 was obtained, positioning FDI as a very good classifier. The optimal cut-off value to discriminate between consciousness and unconsciousness based on FDI was set at 3.73 (dotted line in Fig. 7 and red circle in Fig. 9).

Published in : Computer Methods and Programs in Biomedicine (2019), n°175, pp. 129-137
DOI: 10.1016/j.cmpb.2019.04.017
Status : Postprint (Author's version)

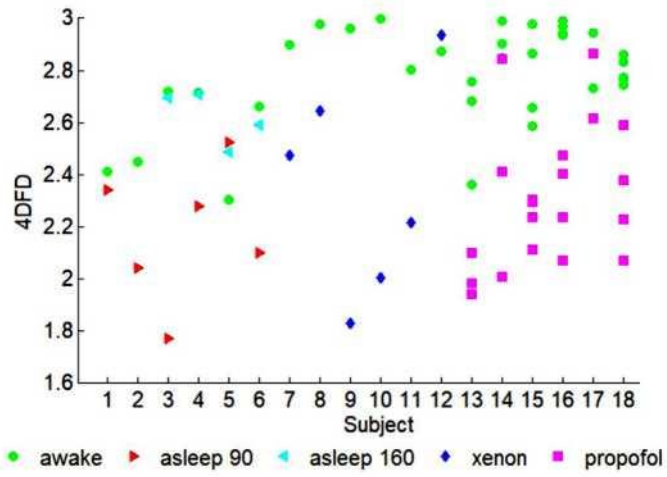

Fig. 5. 4DFD for measurements in the data set, where 4DFD is the 4D FD value for the 4D matrix defined by the point clouds made up of locations of significant sources for all times samples from 8 ms to 130 ms.

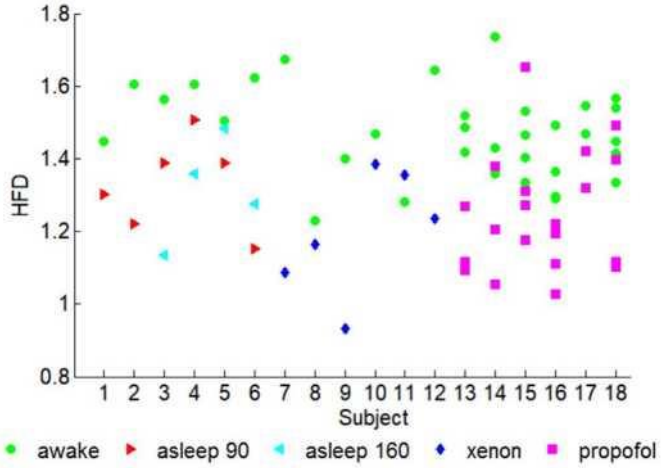

Fig. 6. HFD values for the curves described by the 3DFD values of the point clouds determined by locations of significant sources at time samples from 8 ms to 130 ms for measurements in the data set.

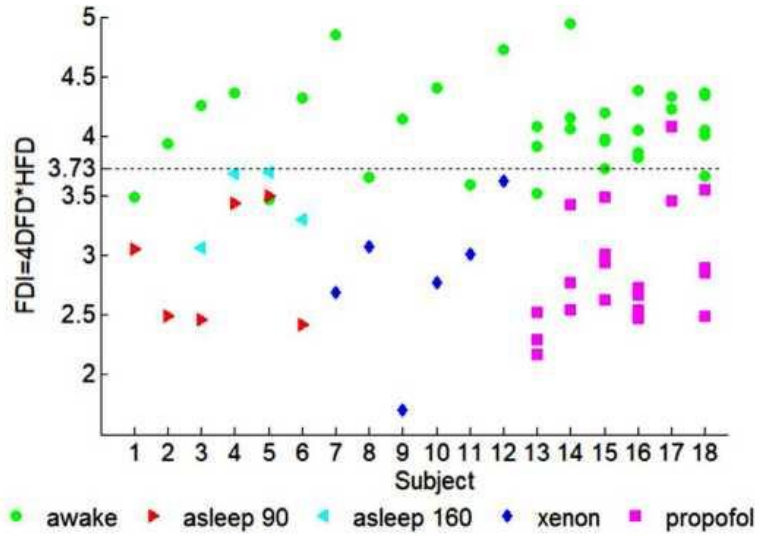

Published in : Computer Methods and Programs in Biomedicine (2019), n°175, pp. 129-137
DOI: 10.1016/j.cmpb.2019.04.017
Status : Postprint (Author's version)

Fig. 7. Fractal Dimension Index for measurements in the data set computed as 4DFD*HFD, where 4DFD is the 4D FD value for the 4D matrix defined by the point clouds made up of locations of significant sources for time samples from 8 ms to 130 ms, and HFD is the Higuchi FD value for the curve described by the 3DFD values of the point clouds determined by locations of significant sources at each time sample from 8 ms to 130 ms. The dotted line at FDI = 3.73 establishes the optimal cut-off value to discriminate between consciousness and unconsciousness according to ROC curve analysis (see Fig. 9).

Table 1

FDI values (mean ± standard deviation) of grouped sessions.

Group	FDI (mean ± std)
Awake	4.08 ± 0.36
Asleep	3.10 ± 0.50
Xenon	2.81 ± 0.63
Propofol	2.87 ± 0.49

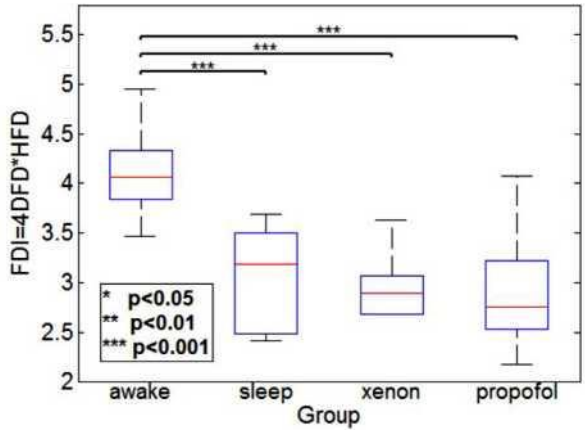

Fig. 8. Boxplot with differences between groups in FDI = 4DFD*HFD. P-values cor-respond to an ANOVA analysis (F = 38.43, p = 2.09x10-14) with post-hoc Bonferroni multiple comparison test. Only p-values below 0.05 are displayed.

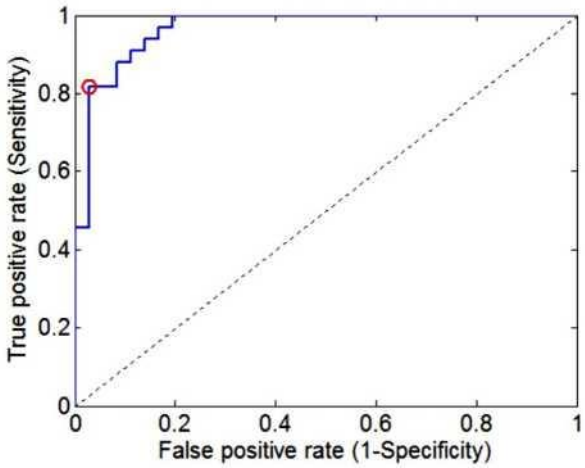

Published in : Computer Methods and Programs in Biomedicine (2019), n°175, pp. 129-137
DOI: 10.1016/j.cmpb.2019.04.017
Status : Postprint (Author's version)

Fig. 9. Receiver operating characteristic (ROC) curve analysis evaluating the performance of classification based on Fractal Dimension Index. The area under ROC curve (AUC) is 0.966. The optimal cut-off value for Fractal Dimension Index is 3.73 (red circle in Figure). (For interpretation of the references to color in this figure legend, the reader is referred to the web version of this article.)

4. Discussion

Recent advances in non-invasive brain imaging have resulted in the proposal of several EEG measures as potential neurophysiological markers of the level of consciousness [3,5,6]. In particular, the spatiotemporal complexity of brain signals as calculated by PCI has so far achieved the best accuracy in detecting consciousness in healthy subjects and brain injured patients [15,16]. Our approach in this paper has been to study the fractal structure of the brain activity and its evolution over time through the FD parameter. Like PCI, we use the brain response to TMS, a non-sensory stimulus. It allows the assessment in patients where standard clinical tests such as CRS-R may fail in detecting consciousness due to patient's inability to respond to a sensory input. Previous studies have analysed the FD of EEG recordings related to consciousness, but always considering the FD of spontaneous EEG. Here, inspired by PCI, we propose a novel method based on analysing the FD of spatiotemporal patterns or cortical activations evoked by TMS.

The FDI is calculated by combining two aspects of the complexity of the brain response to TMS: complexity as a ratio of the change in detail of the spatiotemporal cortical activation to the change of scale (4DFD); and complexity as the variability of the spatial activations over time (HFD). It supposes a measure of the complexity level of the flow of structures evolving after TMS. The 4DFD is sensitive to the dispersion of cortical activation caused by the perturbation, while the HFD of the 3DFD curve captures the complexity of the states the system goes through as it evolves in time. FDI is basically an experimental measure that provides in a single number how the complexity of a dynamical system evolves over time.

Complexity measured with 4DFD is, in general, greater when subjects are awake, especially for the intra-subject case (Fig. 5). This result is consistent with the idea that one expects a more complex distribution of the neuronal activation in a conscious brain. But considering only the 4DFD value fails in two situations: 1) 4DFD values in NREM sleep under high stimulation intensity (asleep 160 in Fig. 5) are very close to or even higher than the 4DFD values in wakefulness; 2) Inter-subject analysis of 4DFD does not allow to clearly discriminate between conscious and unconscious states.

On the other hand, HFD values of sleeping subjects are, in general, lower than HFD when they are awake (see Fig. 6), meaning that the evolution over time of the complexity of the distribution of the brain activity is more complex when subjects are conscious. HFD estimates the complexity of the curve and therefore provides a measure of how complex the 3DFD evolution over time is, and as we stated above it reflects the informational cortical richness at the time of the TMS pulse. As in the case of 4DFD, the inter-subject analysis of HFD cannot discriminate between conscious and unconscious states.

Nevertheless, the problems cited above are overcome by combining 4DFD and HFD in FDI: 1) FDI values of sessions in unconscious state with different stimulus intensity are clearly

Published in : Computer Methods and Programs in Biomedicine (2019), n°175, pp. 129-137
DOI: 10.1016/j.cmpb.2019.04.017
Status : Postprint (Author's version)

separated from the corresponding sessions in conscious state (see subjects 3 to 6 in Fig. 7) with only one exception; 2) FDI performs very well as a classifier (Figs. 7-9) with an optimal cut-off value of FDI = 3.73 separating consciousness from unconsciousness with very few exceptions. Moreover, FDI results were similar when subjects were sleeping or sedated through the anaesthetics xenon and propofol, which have different mechanisms of action. This fact suggests that the fractal analysis of brain activity after TMS summarized in FDI captures a neural correlate of the level of consciousness in healthy individuals that is general and reliable. The characteristics of the corticothalamic system that FDI estimates are both the structural complexity and its variability. They are sensitive to the fractal structure of the brain's response to a magnetic perturbation. Since FDI assesses the early response generated through deterministic interactions within the thalamocortical system to TMS, the resulting measured complexity is minimally affected by random processes (noise or muscle activity) present when longer periods of time are evaluated [12].

Roughly speaking, we can say that brain activity in consciousness presents both a structure and an evolution over time more complex than in unconsciousness. Both pieces of information are related to the IIT theory of consciousness. Accordingly to IIT, consciousness requires a critical balance between integration and differentiation of the thalamocortical networks. Such integrated systems with a large repertoire of informational structures generated by their parts are expected to respond to TMS with widespread patterns of activity and a large variety of different states. In this perspective, FDI would be related to those theoretical measures of brain complexity that explicitly aim at quantifying the conjoint presence of functional integration and functional differentiation in neural systems, although we have to note that FDI does not aim to validate IIT, neither assuming its specific axioms and postulates.

An increasing literature in Theoretical Neuroscience is developing global modelling for whole brain dynamics (see, among others, [26,27,58]. When a dynamical system is settled on a physical substrate described as a complex network, the global attractor always defines a new complex structure, of informational nature, leading to a global transformation of the phase space into an Informational Field [30]. What is now important to note is that the flow of these informational structures and fields is expected to be an evolution of fractal networks, due to both the complexity of the physical substrate and the nonlinearities needed in the modelization process. These (possibly fractal) structures govern the complexity of the real data coming from experiments. This is why it is so crucial, from a theoretical point of view, to obtain indicators related to fractality of the data, as we have done in this study through FDI. In other words, what we expect is that conscious states should be discriminated by a categorization of their associated informational structures and informational fields, with the FDI being a key measure for this aim. The main hypothesis underlying FDI is that consciousness depends on the ability of many functionally specialized modules of the thalamocortical system to interact rapidly and effectively. We certainly have strong evidence supporting this hypothesis [15,16,38,59]. We assume that this approach is still in its infancy, and we are now searching for experimental evidence of the discrimination of these states of consciousness, and for a proper description of informational structures from real time series data.

Ahead of PCI, the power of FDI as a classifier was very good but did not reach a completely disjoint separation between wakefulness and unconsciousness. The main limitation of FDI

Published in : Computer Methods and Programs in Biomedicine (2019), n°175, pp. 129-137
DOI: 10.1016/j.cmpb.2019.04.017
Status : Postprint (Author's version)

compared to PCI is not being able to handle time periods where there is no significant response. 4DFD measures the fractal dimension of the point clouds defined by the locations of sources that are significantly activated by TMS, and thus needs a large enough number of those locations to be computed. This number of significant sources decreases drastically by about 130 ms after the TMS for the case of sleep sessions, hence the analysis was restricted to this early component of the TMS response. This situation implies discarding complex activations that are present in wakefulness after this time period. Taking into account that FD is a quite robust measure in the presence of noise [60], future studies could consider using less restrictive binarization procedures in order to allow reliable fractal analyses to be performed over larger periods of time.

On the other hand, FDI appears to have certain advantages with respect to PCI. The first one is that FDI gives more information than PCI does: FDI is constructed as a product between an integration FD (4DFD) and a differentiation FD (HFD). So FDI provides not only the complete picture but also the different aspects of spatiotemporal complexity, while PCI needs other measures, such as Significant Current Density and Significant Current Scattering to better characterize responses [40,59]. Moreover, FDI could be calculated by regions of interest in the brain. Similar computation can certainly be performed with PCI, but since PCI is based on algorithmic complexity the relation between the whole and its parts would be difficult to infer. Instead, FDI could be adapted to evaluate contributions from different areas of the brain to the overall spatiotemporal complexity. This could be particularly relevant to study conditions such as strokes and a minimally conscious state, in which patients may have portions of the cortex that are normal and other areas that are damaged.

Previous studies [15,16] showed that the complexity of large- scale spatiotemporal patterns of cortical activation in response to the TMS is robust across subjects and independent on stimulated area and stimulation intensity. In agreement with those findings, our FDI results did not present significant differences between stimulation sites or intensities either. To the extent that FDI quantifies this large-scale complexity, it should be largely insensitive to the stimulated area and cortical architecture. Nevertheless, future studies employing a larger number of subjects in different conditions are needed to test this hypothesis and to increase the statistical power of the analyses.

Further studies are also needed to analyse how FDI performs in conditions where loss of consciousness is present such as brain- injured patients who have emerged from coma and subjects who are behaviourally unresponsive yet conscious.

5. Conclusions

Our results suggest that the fractal dimension of brain activations evoked by TMS may be a sensitive method for characterizing consciousness states in healthy individuals without requiring the subjects to perform any sensory, motor, or cognitive tasks. In this regard, FDI appears to be a theoretically-rooted and promising tool for obtaining a deeper understanding of the relationship between consciousness and brain complexity.

Published in : Computer Methods and Programs in Biomedicine (2019), n°175, pp. 129-137
DOI: 10.1016/j.cmpb.2019.04.017
Status : Postprint (Author's version)

Acknowledgments

This work has been partially supported by the Spanish Government and the European Union (via ERDF funds) through the research project MTM2014-61312-EXP. A.G.C. was supported by São Paulo Research Foundation, grant 2016/08263-9.

Conflict of interest

The authors declare that they have no conflict of interest.

References

[1] S. Dehaene, J.-P. Changeux, Experimental and theoretical approaches to conscious processing, Neuron 70 (2011) 200-227, doi:10.1016/j.neuron.2011.03.018.

[2] O. Bodart, O. Gosseries, S. Wannez, A. Thibaut, J. Annen, M. Boly, M. Rosanova, A.G. Casali, S. Casarotto, G. Tononi, M. Massimini, S. Laureys, Measures of metabolism and complexity in the brain of patients with disorders of consciousness, NeuroImage Clin. 14 (2017) 354-362, doi:10.1016/j.nicl.2017.02.002.

[3] C. Koch, M. Massimini, M. Boly, G. Tononi, Neural correlates of consciousness: progress and problems, Nat. Rev. Neurosci. 17 (2016) 307-321, doi:10.1038/nrn. 2016.61.

[4] A.K. Seth, Z. Dienes, A. Cleeremans, M. Overgaard, L. Pessoa, Measuring consciousness: relating behavioural and neurophysiological approaches, Trends Cogn. Sci. 12 (2008) 314-321, doi:10.1016/j.tics.2008.04.008.

[5] J.D. Sitt, J.R. King, I. El Karoui, B. Rohaut, F. Faugeras, A. Gramfort, L. Cohen, M. Sigman, S. Dehaene, L. Naccache, Large scale screening of neural signatures of consciousness in patients in a vegetative or minimally conscious state, Brain 137 (2014) 2258-2270, doi:10.1093/brain/awu141.

[6] D.A. Engemann, F. Raimondo, J.R. King, B. Rohaut, G. Louppe, F. Faugeras, J. Annen, H. Cassol, O. Gosseries, D. Fernandez-Slezak, S. Laureys, L. Naccache, S. Dehaene, J.D. Sitt, Robust EEG-based cross-site and cross-protocol classification of states of consciousness, Brain 141 (2018) 3179-3192, doi:10.1093/brain/ awy251.

[7] J.T. Giacino, K. Kalmar, J. Whyte, The JFK Coma Recovery Scale-Revised: measurement characteristics and diagnostic utility, Arch. Phys. Med. Rehabil. 85 (2004) 2020-2029, doi:10.1016/J.APMR.2004.02.033.

[8] A.M. Goldfine, J.D. Victor, M.M. Conte, J.C. Bardin, N.D. Schiff, Determination of awareness in patients with severe brain injury using EEG power spectral analysis, Clin. Neurophysiol. 122 (2011) 2157-2168, doi:10.1016/j.clinph.2011.03.022.

[9] G. Untergehrer, D. Jordan, E.F. Kochs, R. Ilg, G. Schneider, Fronto-parietal connectivity is a non-static phenomenon with characteristic changes during un-consciousness, PLoS One 9 (2014), doi:10.1371/journal.pone.0087498.

[10] S. Beukema, L.E. Gonzalez-Lara, P. Finoia, E. Kamau, J. Allanson, S. Chennu, R.M. Gibson, J.D. Pickard, A.M. Owen, D. Cruse, A hierarchy of event-related potential markers of auditory processing in disorders of consciousness, NeuroImage Clin. 12 (2016) 359-371, doi:10.1016/j.nicl.2016.08.003.

[11] A. Thul, J. Lechinger, J. Donis, G. Michitsch, G. Pichler, E.F. Kochs, D. Jordan,

Published in : Computer Methods and Programs in Biomedicine (2019), n°175, pp. 129-137
DOI: 10.1016/j.cmpb.2019.04.017
Status : Postprint (Author's version)

R. Ilg, M. Schabus, EEG entropy measures indicate decrease of cortical information processing in disorders of consciousness, Clin. Neurophysiol. 127 (2016) 1419-1427, doi:10.1016/j.clinph.2015.07.039.

[12] R. Ferenets, T. Lipping, A. Anier, V. Jântti, S. Melto, S. Hovilehto, Comparison of entropy and complexity measures for the assessment of depth of sedation, IEEE Trans. Biomed. Eng. 53 (2006) 1067-1077, doi:10.1109/TBME.2006.873543.

[13] M. Jospin, P. Caminal, E.W. Jensen, H. Litvan, M. Vallverdu, M.M.R.F. Struys, H.E.M. Vereecke, D.T. Kaplan, Detrended fluctuation analysis of EEG as a measure of depth of anesthesia, IEEE Trans. Biomed. Eng. 54 (2007) 840-846, doi:10.1109/TBME.2007.893453.

[14] M. Schartner, A. Seth, Q. Noirhomme, M. Boly, M.A. Bruno, S. Laureys, A. Barrett, Complexity of multi-dimensional spontaneous EEG decreases during propofol induced general anaesthesia, PLoS One 10 (2015), doi:10.1371/journal. pone.0133532.

[15] A.G. Casali, O. Gosseries, M. Rosanova, M. Boly, S. Sarasso, K.R. Casali,

S. Casarotto, M.-A. Bruno, S. Laureys, G. Tononi, M. Massimini, A theoreti¬cally based index of consciousness independent of sensory processing and behavior, Sci. Transl. Med. 5 (2013) 198ra105-198ra105, doi:10.1126/scitranslmed. 3006294.

[16] S. Casarotto, M. Rosanova, O. Gosseries, M. Boly, M. Massimini, S. Sarasso, Exploring the neurophysiological correlates of loss and recovery of consciousness: perturbational complexity, in: M.M. Monti, W.G. Sannita (Eds.), Brain Funct. Responsiveness Disord. Conscious, Springer International Publishing, Cham, 2016, pp. 93-104, doi:10.1007/978-3-319-21425-2_8.

[17] M. Oizumi, L. Albantakis, G. Tononi, From the phenomenology to the mechanisms of consciousness: integrated information theory 3.0, PLoS Comput. Biol. 10 (2014), doi:10.1371/journal.pcbi.1003588.

[18] G. Tononi, Consciousness as integrated information: a provisional manifesto, Biol. Bull. 215 (2008) 216-242 doi:215/3/216 [pii].

[19] G. Werner, Fractals in the nervous system: conceptual implications for theoretical neuroscience, Front. Physiol. (1 JUL) (2010), doi:10.3389/fphys.2010.00015.

[20] R. Lopes, N. Betrouni, Fractal and multifractal analysis: a review, Med. Image Anal. 13 (2009) 634-649, doi:10.1016/j.media.2009.05.003.

[21] B.B. Mandelbrot, The fractal geometry of nature, 1983. doi:10.1119/1.13295.

[22] X. Li, J. Polygiannakis, P. Kapiris, A. Peratzakis, K. Eftaxias, X. Yao, Fractal spectral analysis of pre-epileptic seizures in terms of criticality, J. Neural Eng. 2 (2005) 11-16, doi:10.1088/1741-2560/2/2/002.

[23] E. Pereda, A. Gamundi, R. Rial, J. Gonzalez, Non-linear behaviour of human EEG: fractal exponent versus correlation dimension in awake and sleep stages, Neurosci. Lett. 250 (1998) 91-94, doi:10.1016/S0304-3940(98)00435-2.

[24] M.J. Woyshville, J.R. Calabrese, Quantification of occipital EEG changes in Alzheimer's disease utilizing a new metric: the fractal dimension, Biol. Psychiatry 35 (1994) 381-387, doi:10.1016/0006-3223(94)90004-3.

[25] N. Brunel, X.J. Wang, Effects of neuromodulation in a cortical network model of object working memory dominated by recurrent inhibition, J. Comput. Neurosci. 11 (2001) 63-85, doi:10.1023/A:1011204814320.

[26] G. Deco, V.K. Jirsa, Ongoing cortical activity at rest: criticality, multistability, and ghost attractors, J. Neurosci. 32 (2012) 3366-3375, doi:10.1523/JNEUROSCI. 2523-11.2012.

Published in : Computer Methods and Programs in Biomedicine (2019), n°175, pp. 129-137
DOI: 10.1016/j.cmpb.2019.04.017
Status : Postprint (Author's version)

[27] J. Cabral, M.L. Kringelbach, G. Deco, Exploring the network dynamics underlying brain activity during rest, Prog. Neurobiol. 114 (2014) 102-131, doi:10.1016/ j.pneurobio.2013.12.005.

[28] G. Guerrero, J.A. Langa, A. Suarez, Attracting Complex Networks, in: Lect. Notes Econ. Math. Syst., 683, 2016, pp. 309-327, doi:10.1007/978-3-319-40803-3_12.

[29] G. Guerrero, J.A. Langa, A. Suarez, Architecture of attractor determines dynamics on mutualistic complex networks, Nonlinear Anal. Real World Appl. 34 (2017) 17-40, doi:10.1016/j.nonrwa.2016.07.009.

[30] FJ. Esteban, J. Galadî, J.A. Langa, J.R. Portillo, Soler-Toscano, Informational Structures: a dynamical system approach for Integrated Information, PLoS Comput. Biol. 14 (2018) 1-33.

[31] M.W. Hirsch, S. Smale, R.L. Devaney, Differential equations, dynamical systems, and an introduction to chaos, 2013. doi:10.1016/C2009-0-61160-0.

[32] X. Nan, X. Jinghua, The fractal dimension of eeg as a physical measure of conscious human brain activities, Bull. Math. Biol. 50 (1988) 559-565, doi:10.1016/ S0092-8240(88)80009-0.

[33] P. Grassberger, Generalized dimensions of strange attractors, Phys. Lett. A. 97 (1983) 227-230, doi:10.1016/0375-9601(83)90753-3.

[34] S. Solhjoo, A.M. Nasrabadi, M.R.H. Golpayegani, EEG-based mental task classification in hypnotized and normal subjects, in: 2005 IEEE Eng. Med. Biol. 27th Annu. Conf., 2005, pp. 2041-2043, doi:10.1109/IEMBS.2005.1616858.

[35] T. Higuchi, Approach to an irregular time series on the basis of the fractal theory, Phys. D Nonlinear Phenom. 31 (1988) 277-283, doi:10.1016/0167-2789(88) 90081-4.

[36] R. Esteller, G. Vachtsevanos, J. Echauz, B. Litt, A Comparison of waveform fractal dimension algorithms, IEEE Trans. Circuits Syst. I Fundam. Theory Appl. 48 (2001) 177-183, doi:10.1109/81.904882.

[37] A.J. Ibânez-Molina, S. Iglesias-Parro, Fractal characterization of internally and externally generated conscious experiences, Brain Cogn. 87 (2014) 69-75, doi:10.1016/j.bandc.2014.03.002.

[38] M. Massimini, F. Ferrarelli, R. Huber, S.K. Esser, H. Singh, G. Tononi, Breakdown of cortical effective connectivity during sleep, Science 309 (2005) 2228-2232 (80-.)., doi:10.1126/science.1117256.

[39] M. Massimini, F. Ferrarelli, M.J. Murphy, R. Huber, B.A. Riedner, S. Casarotto, G. Tononi, Cortical reactivity and effective connectivity during REM sleep in humans REM sleep in humans, Cogn. Neurosci. 1 (2010) 176-183, doi:10.1080/ 17588921003731578.

[40] A.G. Casali, S. Casarotto, M. Rosanova, M. Mariotti, M. Massimini, General indices to characterize the electrical response of the cerebral cortex to TMS, Neuroimage 49 (2010) 1459-1468, doi:10.1016/j.neuroimage.2009.09.026.

[41] P. Berg, M. Scherg, A fast method for forward computation of multiple-shell spherical head models, Electroencephalogr. Clin. Neurophysiol. 90 (1994) 58¬64, doi:10.1016/0013-4694(94)90113-9.

[42] Z. Zhang, A fast method to compute surface potentials generated by dipoles within multilayer anisotropic spheres, Phys. Med. Biol. 40 (1995) 335-349, doi:10.1088/0031-9155/40/3/001.

[43] K. Friston, R. Henson, C. Phillips, J. Mattout, Bayesian estimation of evoked and induced responses, Hum. Brain Mapp. 27 (2006) 722-735, doi:10.1002/hbm. 20214.

[44] J. Mattout, C. Phillips, W.D. Penny, M.D. Rugg, K.J. Friston, MEG source localization under multiple constraints: an extended Bayesian framework, Neuroimage 30 (2006) 753-767, doi:10.1016/j.neuroimage.2005.10.037.

Published in : Computer Methods and Programs in Biomedicine (2019), n°175, pp. 129-137
DOI: 10.1016/j.cmpb.2019.04.017
Status : Postprint (Author's version)

[45] C. Phillips, J. Mattout, M.D. Rugg, P. Maquet, K.J. Friston, An empirical Bayesian solution to the source reconstruction problem in EEG, Neuroimage 24 (2005) 997-1011, doi:10.1016/j.neuroimage.2004.10.030.

[46] J. Ruiz de Miras, J. Navas, P. Villoslada, F.J. Esteban, UJA-3DFD, A program to compute the 3D fractal dimension from MRI data, Comput. Methods Programs Biomed. (2011) 104, doi:10.1016/j.cmpb.2010.08.015.

[47] J. Ruiz de Miras, Fractal analysis in MATLAB: a tutorial for neuroscientists, in: A. Di Ieva (Ed.), Fractal Geom. Brain, Springer New York, New York, NY, 2016, pp. 523-532., doi:10.1007/978-1-4939-3995-4_33.

[48] S. Selvam, T. Nadu, Complete Higuchi Fractal Dimension Algorithm, (2013). https://www.mathworks.com/matlabcentral/fileexchange/ 30119- complete- higuchi- fractal-dimension- algorithm.

[49] T.L.A. Doyle, Discriminating between elderly and young using a fractal dimension analysis of centre of pressure, Int. J. Med. Sci. 11 (2004), doi:10.7150/ijms.

1.11.

[50] C. Gômez, A. Mediavilla, R. Hornero, D. Abâsolo, A. Fernândez, Use of the Higuchi's fractal dimension for the analysis of MEG recordings from Alzheimer's disease patients, Med. Eng. Phys. 31 (2009) 306-313, doi:10.1016/ j.medengphy.2008.06.010.

[51] R.a McLean, W.L. Sanders, W.W. Stroup, A unified approach to mixed linear models, Am. Stat. 45 (1991) 54-64, doi:10.2307/2685241.

[52] R.I. Jennrich, M.D. Schluchter, Unbalanced repeated-measures models with structured covariance matrices, Biometrics 42 (1986) 805-820, doi:10.2307/ 2530695.

[53] O.J. Dunn, Multiple comparisons among means, J. Am. Stat. Assoc. 56 (1961) 52, doi:10.2307/2282330.

[54] D.M. Green, J.A. Swets, Signal detection theory and psychophysics, 1966.

[55] J.A. Hanley, B.J. McNeil, The meaning and use of the area under a receiver op¬erating characteristic (ROC) curve, Radiology 143 (1982) 29-36, doi:10.1148/ radiology.143.1.7063747.

[56] N.J. Perkins, E.F. Schisterman, The inconsistency of "optimal" cutpoints obtained using two criteria based on the receiver operating characteristic curve, Am. J. Epidemiol. 163 (2006) 670-675, doi:10.1093/aje/kwj063.

[57] R. Bettinger, Cost-sensitive classifier selection using the ROC convex hull method, in: A. Braverman (Ed.), Comput. Sci. Stat., Interface Foundation of North America, 2003, pp. 142-153.

[58] G. Deco, G. Tononi, M. Boly, M.L. Kringelbach, Rethinking segregation and integration: contributions of whole-brain modelling, Nat. Rev. Neurosci. 16 (2015) 430-439, doi:10.1038/nrn3963.

[59] F. Ferrarelli, M. Massimini, S. Sarasso, A. Casali, B.A. Riedner, G. Angelini, G. Tononi, R.A. Pearce, Breakdown in cortical effective connectivity during midazolam-induced loss of consciousness, Proc. Natl. Acad. Sci. 107 (2010) 2681-2686, doi:10.1073/pnas.0913008107.

[60] G.E. Polychronaki, P.Y. Ktonas, S. Gatzonis, A. Siatouni, P.A. Asvestas, H. Tsekou, D. Sakas, K.S. Nikita, Comparison of fractal dimension estimation algorithms for epileptic seizure onset detection, J. Neural Eng. 7 (2010) 046007, doi:10. 1088/1741-2560/7/4/046007.